JOURNAL OF GEOPHYSICAL RESEARCH, VOL. 102, NO. B10, PAGES 22,671–22,680, OCTOBER 10, 1997

Determination of the preexponential frequency factor for superparamagnetic maghemite particles in magnetoferritin

Bruce M. Moskowitz,[1] Richard B. Frankel,[2] Sarah A. Walton,[3] Dominic P. E. Dickson,[3] K. K. W. Wong,[4] T. Douglas,[4] and Stephen Mann[4]

Abstract. Magnetization and Mössbauer measurements on maghemite particles with an average particle diameter of 10 nm have been made in the temperature range from 5 K to 353 K spanning the superparamagnetic (SPM) and stable single domain (SD) regimes. The maghemite particles were produced within the iron-storage protein ferritin, resulting in a narrowly-sized, weakly interacting nanocomposite material called magnetoferritin. Experiments combining hysteresis measurements, low temperature remanence, and Mössbauer spectroscopy were used to characterize magnetoferritin and to provide experimental estimates of (1) the pre-exponential frequency factor f_0 in the Néel-Arhennius relaxation equation; (2) the SPM threshold size at room temperature for maghemite; and (3) the SD value of H_r/H_c at 0 K. The frequency factor was determined from the difference in blocking temperatures measured by dc magnetization and Mössbauer spectroscopy, yielding a value of $f_0 \approx 10^9$ Hz. This agrees well with the standard value and justifies the usually assumed superparamagnetic blocking condition of KV=25 kT for remanence measurements. The SPM threshold size at room temperature for remanence measurements was estimated to be 20-27 nm and the extrapolated SD value at 0 K for H_r/H_c is 1.32. The latter value is slightly larger than the theoretical value of 1.09 but may be more appropriate for weakly interacting SD particles commonly found in sediments and soils. However, f_0 for ferrimagnetic magnetoferritin is a factor of 10^3 lower than was determined previously for native ferritin, which contains antiferromagnetic ferrihydrite cores. The difference in f_0 values between the two varieties of ferritin is probably related to the two different types of magnetic spin ordering of the core minerals and suggests that the higher value of f_0 is more appropriate for antiferromagnetic minerals like hematite and goethite, whereas the lower value is more appropriate for ferrimagnetic minerals like maghemite, magnetite, or greigite.

1. Introduction

The theory of thermal activation in small, magnetically ordered grains developed by *Néel* [1949] continues to be one of the main theoretical foundations of rock magnetism [*Stacey and Banerjee*, 1974]. For example, Néel's theory provides the theoretical justification in paleomagnetism for interpreting characteristic directions in ancient rocks as primary magnetizations, for demagnetization techniques to remove secondary magnetizations, and for paleointensity methods [e.g., *Dunlop*, 1995]. In the original Néel model, each grain is considered to be a non interacting, uniformly magnetized single domain (SD) particle with an anisotropy energy barrier (ΔE_B) separating stable states of magnetization. If the particle is small enough, ΔE_B can become comparable to the thermal energy and thermal activation over the energy barrier produces spontaneous changes in the direction of magnetization, resulting in magnetic relaxation phenomena such as superparamagnetism, magnetic viscosity, magnetic blocking, and thermoremanent magnetization [*Néel*, 1949; *Bean and Livingston*, 1959, *Dunlop*, 1973]. More recently, the identification of superparamagnetic (SPM) grains in a variety of sediments, soils, and submarine basalt glasses, or produced by bacteria [*Moskowitz et al.*, 1989; *Banerjee et al.*, 1993; *Tarduno*, 1995; *Tauxe et al.*, 1996] has renewed interest in the theory of superparamagnetism.

In this paper, we present a study of the magnetic properties of superparamagnetic maghemite (γ-Fe_2O_3) below 300 K. Narrowly sized (≈10 nm) maghemite particles were produced within the iron-storage protein ferritin. Natural ferritin consists of a roughly spherical protein shell of 12 nm outer diameter surrounding an 8-nm-diameter cavity containing a core of the mineral ferrihydrite. The native ferrihydrite cores were removed from the protein cavity and replaced by cores of maghemite, yielding the nanocomposite magnetoferritin [*Meldrum et al.*, 1992]. The protein shell acts to keep the mineral soluble and the particles separated, reducing magnetic dipolar interaction effects.

Experiments combining hysteresis measurements, low temperature remanence behavior, and Mössbauer spectro-

[1]Department of Geology and Geophysics, Institute for Rock Magnetism, University of Minnesota, Minneapolis.
[2]Physics Department, California Polytechnic State University, San Luis Obispo.
[3]Department of Physics, University of Liverpool, Liverpool, England, United Kingdom.
[4] School of Chemistry, University of Bath, Bath, England, United Kingdom.

Paper number 97JB01698.
0148-0227/97/97JB-01698$09.00

scopy were used to characterize magnetoferritin and to provide an experimental estimate of the Néel frequency factor f_0 for the maghemite cores. This constant has been estimated to be in the range of 10^8-10^{13} Hz [*Néel*, 1949; *Brown*, 1959] but is usually taken as 10^9 Hz [e.g., *Moon and Merrill*, 1988]. The frequency factor is an important parameter in Néel's SD theory because it determines the timescale for stability of remanence and sets the size limit for SPM behavior. Yet few experimental determinations of this constant for SD materials are available [e.g., *McNab et al.*, 1968; *Xiao et al.*, 1986; *Dickson et al.*, 1993]. Our approach follows the methods described by *Dickson et al.* [1993] for ferrihydrite cores in natural ferritin and by *Xiao et al.* [1986] for Fe-(SiO_2) granular films. It combines magnetometry and Mössbauer spectroscopy to measure blocking temperatures at two different characteristic measuring times. Our results also provide an estimate of the SPM-SD transition size at room temperature for maghemite and the single domain value of H_r/H_c.

2. Theory

The switching or superparamagnetic relaxation time τ for magnetization reversal over an anisotropy barrier is given by the Néel-Arrhenius equation

$$\tau^{-1} = f_0 \exp(-\Delta E_B/kT) \quad (1)$$

where k is the Boltzmann constant, T is the absolute temperature, and f_0 is the preexponential frequency factor. For a Stoner-Wohlfarth particle with uniaxial anisotropy and the easy axis perfectly aligned with the applied field H, $\Delta E_B = KV[1 \pm H/H_K]^2$, where K is the anisotropy constant, V is particle volume, and $H_K = 2K/\mu_0 M_s$ is the anisotropy field for coherent switching of magnetization [*Stoner and Wohlfarth*, 1948]. In contrast to the exponential term in (1), the frequency factor f_0, which is the subject of this paper, is weakly dependent upon temperature, anisotropy, and particle volume and is related to the natural gyromagnetic precessional frequency of dipole spins in an anisotropy field. At the blocking temperature T_b, the relaxation time in (1) equals the characteristic time t of the measurement, and particles become superparamagnetic. For a typical dc remanence measurement with t=100 s and H=0, setting $\tau = t$ in (1) gives the critical volume, V_{sp}, for SPM behavior [*Bean and Livingston*, 1959]

$$KV_{sp} = kT_b \ln(f_0 t) \quad (2)$$

In most particle systems, including natural samples, there exists a distribution of particle volumes which leads to a distribution in blocking temperatures. The median blocking temperature is defined as the temperature at which half the particle volumes are in the SPM state and depends on the timescale of the measurement (e.g., dc remanence, ac susceptibility, or Mössbauer spectroscopy). At temperatures above T_b, the magnetization curve for an assembly of identical, noninteracting SPM particles exhibits no remanence M_r or coercivity H_c and is given by the classical Langevin function

$$M(T,H) = M_s[\coth(\mu_0 \mu H/kT) - kT/\mu_0 \mu H] \quad (3)$$

where M_s is the saturation magnetization, μ is the dipole moment per particle (equal to VM_s), and $KV/kT \ll 1$. Fitting isothermal M-H curves to (3), usually assuming a lognormal or uniform distribution of dipole moments, yields a mean SPM particle size and, together with an estimate of T_b and (2), the effective anisotropy constant.

Below T_b, particles are blocked and exhibit hysteresis with H_c and M_r depending on temperature and time. For a random assembly of uniaxial particles, the Stoner-Wohlfarth model can be used to show that the dependence of barrier height on the applied field is $\Delta E_B = KV[1 \pm H/H_K]^{1.43}$, where the exponent in this expression now differs from the standard value of 2 for the special case when the easy axes are collinear with the field direction [*Pfeiffer*, 1990]. The measured H_c is the value of H which makes $\tau = t$ in (1) and is given by

$$H_c(T,t) = H_{c0}[1 - (kT \ln(f_0 t)/KV)^{0.7}] \quad (4)$$

where $H_{c0} \approx H_K/2$ and is the mean coercivity at T=0 K. The bulk coercivity or the remanent coercivity H_r can be used in (4) as a measure of the mean coercivity. Equation (4) is the basic equation of thermal fluctuation analysis [*Dunlop*, 1976] but modified to account for the random orientation of uniaxial easy axes. Experimental measurement of the temperature dependence of H_c or H_r provides additional, independent estimates of V and K.

3. Experimental Methods

Magnetoferritin was prepared as previously described [*Meldrum et al.*, 1992; *Bulte et al.*, 1994]. Repeated increments of 115 Fe(II) ions per protein molecule, followed by stoichiometric amounts of oxidant, were added to the synthesis mixture to give a theoretical final loading of 2300 Fe atoms in each protein cavity. The synthesis was done at 65°-70°C over a period of 5.5 hours.

Magnetoferritin suspensions were deposited on carbon-coated, Formvar-covered copper TEM grids. Bright field images and electron diffraction patterns were recorded. Particle size distributions were measured from enlarged micrographs. One hundred discrete particles and sixty particles contained within aggregated clusters were measured.

Magnetization measurements were made in fields up to 2.5 T in the temperature range from 5 to 300 K using a SQUID susceptometer (Quantum Design MPMS2). The magnetoferritin suspension was placed in a small plastic holder, and measurements were made either in the frozen state below 250 K or in the liquid state at 300 K. All measurements made in the solid state were done after the sample was frozen in zero field.

Mössbauer spectra were obtained using an ^{57}Co in rhodium source and a conventional constant acceleration spectrometer. The variable low-temperature sample environment was obtained using a continuous flow cryostat (Oxford Instruments Ltd., CF500) and temperature controller (Oxford Instruments Ltd., ITC4) with temperature measured using a calibrated carbon in glass resistance thermometer and an ac resistance bridge (Automatic Systems Laboratory). Applied magnetic field measurements up to 14 T were made using a superconducting magnet system with the field direction parallel to the gamma ray beam.

4. Results

4.1. Transmission Electron Microscopy (TEM)

A transmission electron micrograph of unstained magnetoferritin is shown in Figure 1. The images showed both discrete mineral cores and small aggregates of the protein

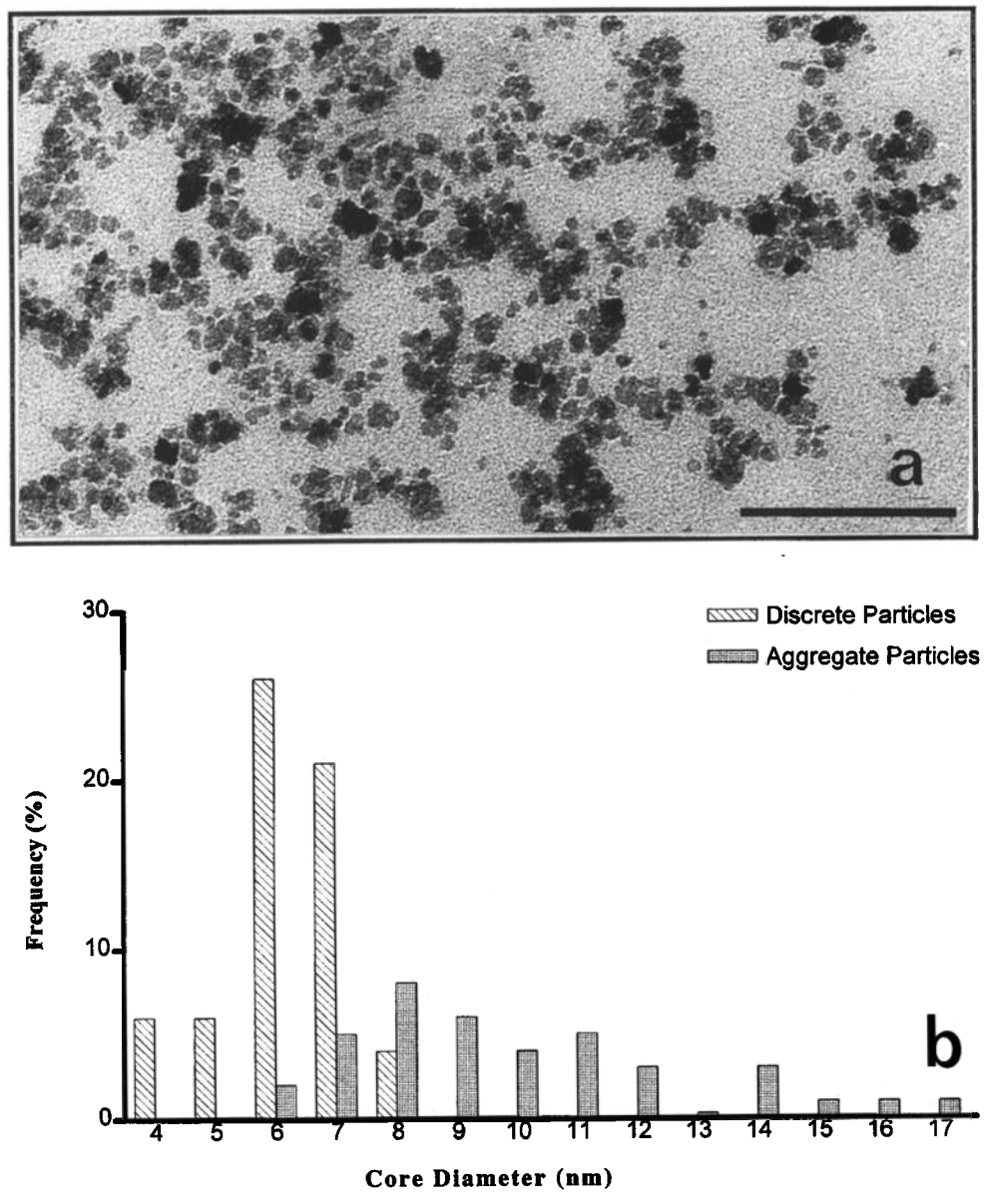

Figure 1. (a) Transmission electron micrograph of unstained magnetoferritin. (b) Particle size distribution plotted as a histogram showing core sizes for both discrete cores and particles associated with the aggregated material. The scale bar in Figure 1a represents 100 nm.

nanoparticles. Native ferritin does not generally agglomerate during air drying onto TEM grids, suggesting that the biomimetic protein is susceptible to protein-protein aggregation. Electron diffraction confirmed a face-centered cubic phase, but it was not possible to distinguish between magnetite and maghemite. Up to seven reflections were usually seen in the electron diffraction patterns, which, considering the small particle size, indicates reasonably good crystallinity. Significant disorder in the cores would have resulted in as few as two lines in the patterns.

Particle sizes were measured for both the discrete cores and for individual cores associated with the larger aggregates on the TEM grid. The former were approximately circular in projection and had dimensions within the range 3 to 7 nm, with a mean diameter of 6 nm and standard deviation (σ) of 1.0 nm (Figure 1b). These nanoparticles are clearly associated with intact protein molecules and reside within the 8-nm cavity of the supramolecular structure. By comparison, the maghemite particles present in the aggregated clusters were often irregular in shape and significantly larger and less monodispersed in size (Figure 1a). The mean size of the individual particles within the clusters was 10 nm (σ=2.6 nm), which is greater than the theoretical diameter of the protein cavity. Particles above 10 nm were irregular but mainly isotropic. Some may have octahedral outlines but were not very well defined at this small size.

One possible explanation for this bimodal distribution of particles sizes is that the maghemite cores outgrow the protein cage by crystallization within the molecular channels that permeate the polypeptide shell. In addition, the protein could be partially damaged by relatively long-term exposure to high temperature during the synthesis procedure.

Alternatively, maghemite particles greater than 10 nm in size might originate from bulk precipitation, although much larger (micrometer) crystals were usually observed in control experiments undertaken without ferritin.

4.2. Mössbauer Spectroscopy

Mössbauer spectra of the magnetoferritin sample obtained in magnetic fields up to 14 T were consistent with previous measurements of magnetoferritin samples that showed the mineral cores to consist of maghemite, γ-Fe_2O_3 [*Pankhurst et al.*, 1994; *Dickson et al.*, 1997]. Spectra were also obtained in zero field over a wide range of temperature, and a representative selection is shown in Figure 2. The 4.2 K spectrum is essentially a magnetically split sextet with a magnetic hyperfine field of 51.5 T. This is slightly but significantly higher than the value of 50 T typically found in native ferritin [*Boas and Window*, 1966; *Bell et al.*, 1984]. However, the value is consistent with that observed for both magnetite and maghemite [e.g., *Kundig and Hargrove*, 1969; *Pankhurst and Pollard*, 1993], although the spectra do not show the degree of structure observed in the spectra of magnetite at this temperature. The lines of the magnetoferritin spectra show a significant degree of broadening and asymmetry, presumably due to the heterogeneity of iron sites, which might be expected in a material with a high surface to volume ratio.

The highest temperature spectrum obtained was at 353 K. This shows a central slightly asymmetric quadrupole-split doublet (isomer shift of 0.27 mm/s and quadrupole splitting of 0.65 mm/s) and a collapsing magnetic sextet. The latter is due to the decreasing sublattice magnetization with increasing temperature. The native ferritin Mössbauer spectrum at temperatures above 50 K shows only a well-defined quadrupole-split doublet (isomer shift of 0.40 mm/s and quadrupole splitting of 0.68 mm/s at 200 K). Thus the spectra of magnetoferritin are significantly different from those of the native ferritin.

The intermediate temperature spectra (e.g., the 200 K spectrum) show the coexistence of doublet and sextet spectral components which is typical of superparamagnetism. The full sextet hyperfine spectrum is observed in magnetically ordered materials when the atomic magnetic moments are fixed in space for a time of 5×10^{-9} s or greater [e.g., *Dickson et al.*, 1993]. A distribution of SPM blocking temperatures leads to characteristic temperature-dependent Mössbauer spectra with the doublet (rapidly relaxing or unblocked) component growing at the expense of the sextet (slowly relaxing or blocked) component as the temperature is increased. This behavior is characterized by a median blocking temperature T_b at which the sextet and doublet components are of equal spectral intensity. The percentage of the total spectral intensity associated with the sextet component as a function of temperature was determined by computer fitting the temperature spectra, and the results show two distinct blocking temperature components (Figure 3). The primary component occurs at T_b=300 K and is taken as the median blocking temperature, whereas a smaller secondary component occurs at T_b=60 K. As is shown below, the 60 K and 300 K blocking temperatures are associated with the discrete cores and the aggregate clusters, respectively. These results are again very different from the value of T_b=36 K obtained for native ferritin [*Dickson et al.*, 1993]. Assuming that the particle sizes are comparable, at least for the discrete cores, this suggests a very different magnetic anisotropy constant for magnetoferritin compared with native ferritin, reflecting the different composition of the mineral cores.

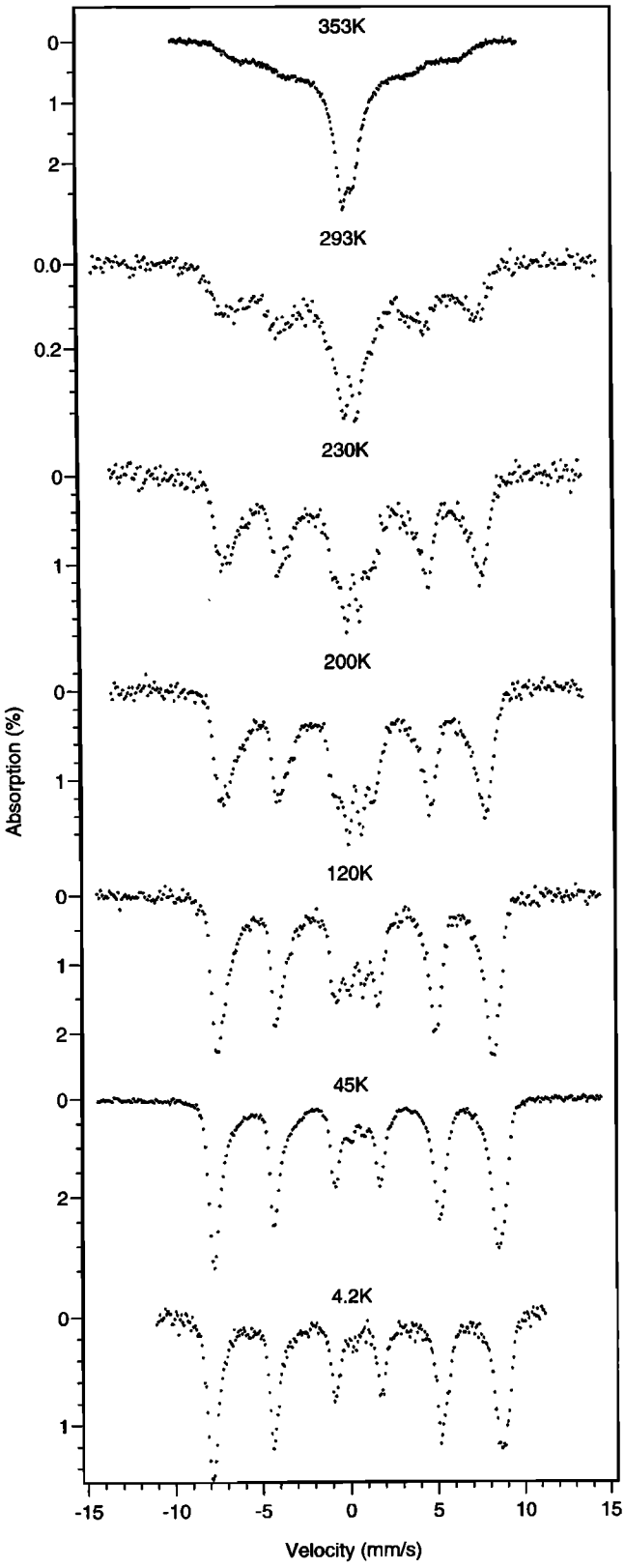

Figure 2. The ^{57}Fe Mössbauer spectra of magnetoferritin obtained in a range of temperatures.

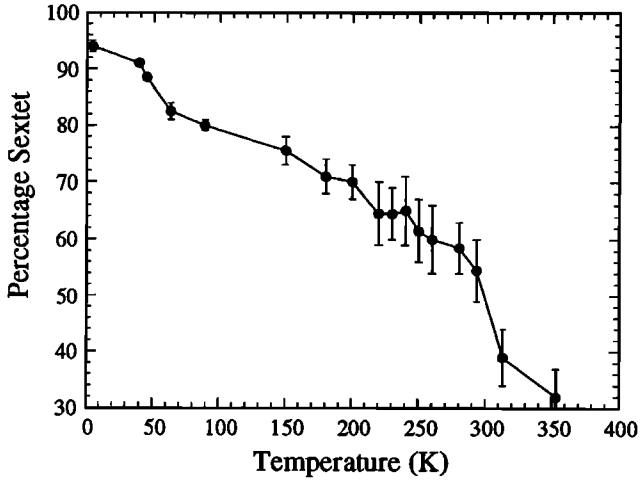

Figure 3. The temperature variation of the total spectral area intensity associated with the sextet component. The sextet and doublet areas were determined from computer fits to the variable temperature magnetoferritin spectra using two different approaches. Each data point is the average of the two different fits, and the error bar is the difference between the two results.

4.3. Room Temperature Magnetization

The field-dependent magnetization of magnetoferritin at 300 K is shown in Figure 4. At 300 K the magnetization saturates but shows no hysteresis, typical of pure SPM behavior. In the liquid state, the physical rotation of the particles into the field direction removes the effects of particle anisotropy on the equilibrium magnetization, thus fulfilling the requirement of $KV/kT<<1$ for a Langevin particle. The 300 K magnetization data were fitted to the function

$$M(T,H)=\frac{M_s}{x}\ln\left[\frac{\sinh x}{x}\right]-\chi H,\quad x=\frac{\mu_0\mu_{max}H}{kT} \qquad (5)$$

in which the first term is obtained by integrating (2) using a uniform distribution of dipole moments from 0 to μ_{max}, and the second term accounts for the diamagnetic/paramagnetic contribution from the water and plastic holder. The results give an mean magnetic moment ($\mu_{max}/2$) of 22,114 Bohr magnetons per magnetoferritin molecule. Since the core is maghemite with a saturation magnetization of 380 kA/m [*Bate*, 1980], the average magnetic moment corresponds to a spherical particle of 10.1 nm diameter, and μ_{max} to a particle of 12.7 nm diameter. Fits using a single-moment or lognormal distribution of dipole moments produced similar results, suggesting a narrow moment distribution and, therefore, a narrow particle volume distribution. The magnetic size of the core determined from (5) is larger than the average core size of the discrete cores (6±1 nm) obtained by TEM but consistent with the average size of the particles in the aggregated material (10±2.6 nm). This suggests that the aggregated material dominates the magnetic behavior at room temperature. From the measured saturation magnetization of the sample, the volume concentration of magnetic material in our sample was 0.16%.

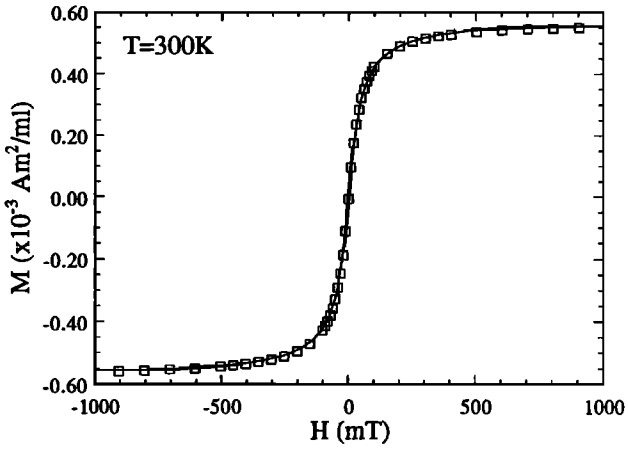

Figure 4. Magnetization as a function of applied field at T=300 K. The solid line is the best fit line to equation (5) in the text.

4.4. Low-Temperature Remanence

Figure 5 shows the temperature decay of a 2.5 T saturation isothermal remanence (SIRM) given at 5 K normalized to the saturation magnetization at 5 K. These data illustrate classical SPM behavior with SIRM rapidly decreasing with increasing temperature as SD particles unblock and become SPM. The median blocking temperature, taken as the temperature where 50% of the remanence has decayed, is T_b=18 K. Above 50 K, magnetization curves show no hysteresis, indicating that the maximum unblocking temperature for the dc measurement is 50 K. Also shown in Figure 5 are M_r/M_s values obtained from hysteresis loops measured at various temperatures, showing that both types of measurements give nearly identical blocking temperature distributions.

4.5. Initial Susceptibility

The temperature dependence of magnetization while warming in a field of 1.5 mT is shown in Figure 6a. The zero field magnetization (ZFM) curve was measured after the

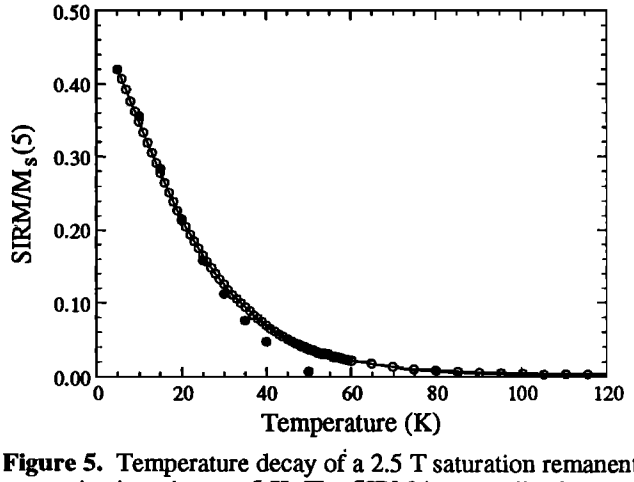

Figure 5. Temperature decay of a 2.5 T saturation remanent magnetization given at 5 K. The SIRM is normalized by the saturation magnetization at 5 K. The solid circles are value of M_r/M_s determined from hysteresis loops at selected temperatures.

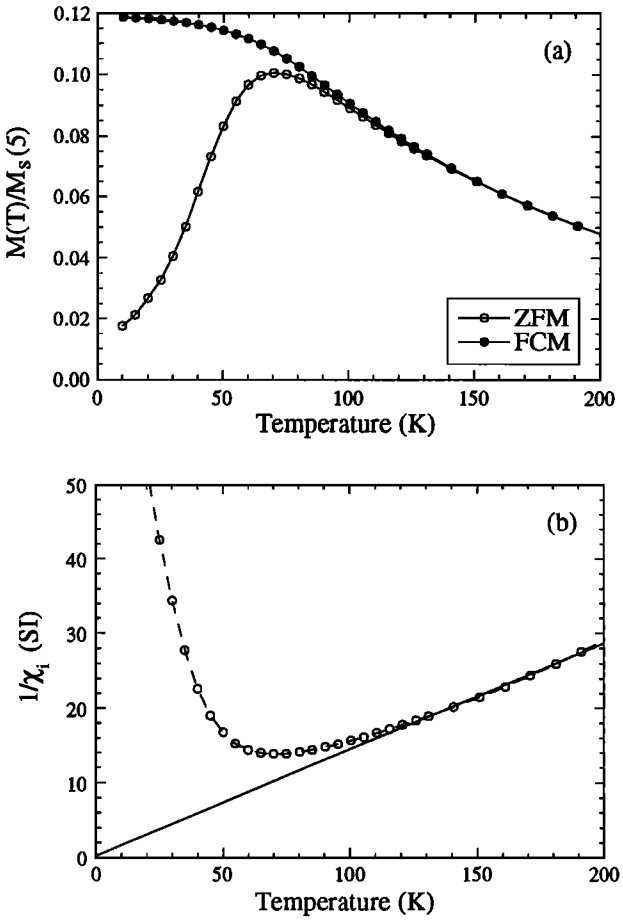

Figure 6. (a) The temperature variation of zero-field magnetization (ZFM) and field-cooled magnetization (FCM) normalized by M_s at 5 K. (b) The temperature variation of the initial dc volume susceptibility (H=1.5 mT) obtained from the ZFM data. The solid line is the best fit to equation (6) in the text.

sample was cooled in zero field (≈0.01 mT) from 240 to 5 K, whereas the field cooled magnetization (FCM) curve was measured after a 1.5 mT field was applied during cooling. In low field, the ZFM curve is proportional to the initial dc susceptibility ($\chi_i=\Delta M/\Delta H$, $H\rightarrow 0$). The peak in the ZFM curve at 70 K is related to the mean blocking temperature of the system and occurs because as the temperature is increased, particles which are initially SD progressively unblock and align their moments with the applied field until, as temperature increases further, thermal energy randomizes the induced magnetization of the unblocked particles [e.g., *Chantrell et al.*, 1991]. In contrast, the FCM curve shows only the demagnetization of blocked particles because the magnetization was already aligned with the field direction during cooling through T_b.

Theoretically, the peak temperature for noninteracting particles is an effective blocking temperature which equals βT_b, where the constant β depends on the form of the particle size distribution with β=1 for a monodispersed distribution and β≈2 for uniform or lognormal distributions [*Gittleman et al.*, 1974]. For β=2, the ZFM data give T_b=35 K, which is a factor of 2 higher than the blocking temperature determined from the decay of SIRM.

At temperatures above the blocking temperature, the ZFM and FCM curves merge as expected in accordance with classical Langevin theory. For magnetically interacting SPM particles, χ_i above T_b usually follows a Curie-Weiss law

$$\chi_i \propto \frac{\mu^2}{T-T_0} \tag{6}$$

where T_0 is an ordering temperature and is usually interpreted as a measure of the strength of particle interactions in the system. Figure 6b shows $1/\chi_i$ versus temperature. Although the data deviate from a simple Curie-Weiss law (partly because of the dependence of μ on temperature), a reasonably linear section is observed for temperatures greater than 120 K, the temperature above which the FCM and ZFM curves merge. The fit to (6) in this temperature range yields a near-zero intercept on the $1/\chi_i$ axis, suggesting that interparticle interactions are weak within this temperature range.

4.6. Magnetostatic Interactions

Evidence for magnetostatic interactions below the blocking temperature in our magnetoferritin sample was obtained from the isothermal remanent magnetization ($I_r(H)$) and the dc demagnetization remanence ($I_d(H)$) curves. In the absence of interaction, the remanence curves are related through the Wohlfarth equation: $I_d(H)=1-2I_r(H)$ [*Wohlfarth*, 1958]. Remanence curves measured at 5 K starting from an initially thermally demagnetized state are shown in Figure 7. The thermally demagnetized state was obtained after the sample had been cooled from 300 K through the blocking temperature in zero field. In Figure 7a the remanence curves are plotted in normalized form as a function of applied field and have a crossover point at a value of 0.43. In Figure 7b the remanence data are plotted as a Henkel plot [*Henkel*, 1964] according to the Wohlfarth equation with the field value as the matching variable. A crossover point different from 0.5 or nonlinearity in the Henkel plot is usually attributed to interparticle dipolar interactions in fine particle systems [*Cisowski*, 1981; *Spratt et al.*, 1988]. The results in Fig. 7 indicate that the interactions are demagnetizing or antiferromagnetic-like. However, the Henkel plot shows that high-field remanences near saturation ($I_r(H)$/SIRM>0.9) merge with the Wohlfarth line, suggesting that SIRM measurements are not affected by interactions.

In our sample, as with other dilute fine particle systems, the interactions are probably related to the formation of particle aggregates, like those observed with TEM (see Figure 1). Magnetic interactions can increase the observed blocking temperature determined from susceptibility measurements because of the dependence of T_b on the height of the energy barrier for magnetization reversal [*El-Hilo et al., 1992*]. Even though the ordering temperature determined from the high-temperature ZFM data is near zero and the volume concentration is low (0.16%), magnetic interactions presumably within the aggregated clusters are still sufficient to cause an anomalous increase in the observed blocking temperature obtained from susceptibility measurements. However, T_b calculated from the decay of high-field saturation remanence (Figure 5) rather than from low-field initial susceptibility (Figure 6) is less affected by interactions and therefore represents a true median blocking temperature, not an effective one [*Chantrell et al.*, 1991]. This is consistent with the results from the Henkel plot (Figure 7b).

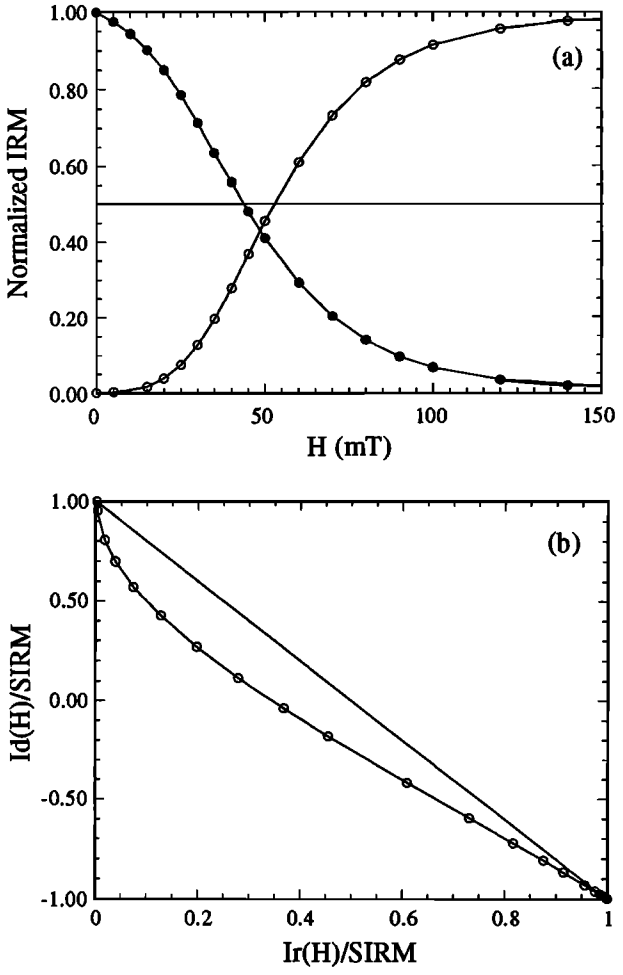

Figure 7. (a) Normalized IRM acquisition and dc demagnetization of SIRM measured at 5 K. IRM curves are normalized to the maximum SIRM. Reversed-field demagnetization curve is rescaled as ½(1+IRM(-*H*)/SIRM). The crossover point occurs at R=0.43. (b) A Henkel plot measured at 5 K with $I_r(H)$/SIRM= normalized IRM acquisition curve and $I_d(H)$/SIRM=normalized dc demagnetization curve. The straight solid line is the theoretical Wohlfarth equation for noninteracting systems.

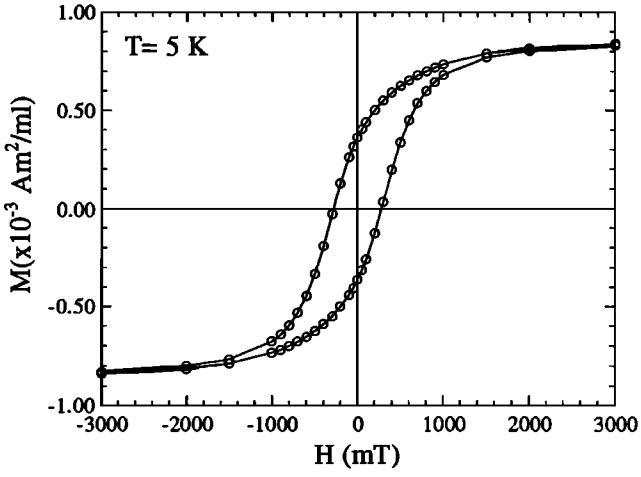

Figure 8. Magnetization as a function of applied field at T=5 K.

4.7. Magnetization Below the Blocking Temperature

Magnetic behavior below 50 K exhibits hysteresis [*Gider et al.*, 1996] as shown in Figure 8. A Day plot of M_r/M_s and H_r/H_c for hysteresis parameters [*Day et al.*, 1977] measured between 5 and 50 K shows a typical power law dependence (Figure 9). The power law dependence results from the change in the proportion of SD and SPM grains as increasing temperature progressively unblocks the SD fraction. The loop shapes do not display constricted or potbellied behavior, even at the highest temperature where hysteresis is still observed. This suggests that either just a very small fraction of SD grains or magnetostatic interactions is sufficient to produce a "normal" SD loop shape [*Tauxe et al.* 1996].

The value of M_r/M_s at 5 K is 0.42 and the extrapolated value at T=0 K is nearly 0.5, the theoretical value for a randomly oriented assemblage of Stoner-Wohlfarth particles with uniaxial anisotropy. However, even at 5 K, the observed M_r/M_s ratio is significantly less than 0.5 and indicates that 16% of the particle distribution is still SPM with blocking temperatures less than 5 K. (The SPM fraction was determined from the M_r/M_s ratio using the relationship $1\text{-}2M_r/M_s$.) From the powerlaw fit on the Day plot (Figure 9), the SD value of H_r/H_c which corresponds to M_r/M_s=0.5 is 1.32, slightly higher than the theoretical value of 1.09 for randomly oriented uniaxial SD particles [*Joffe and Heuberger*, 1974]. A similar value for H_r/H_c was obtained for a magnetite ferrofluid by *Söffge and Schmidbauer* [1981] with a volume concentration approximately 10 times larger than in our sample.

Although the ferritin protein cage is nearly spherical and would seem to impose a multiaxial magnetocrystalline anisotropy on the maghemite core, a uniaxial anisotropy can still develop in these and other nanosized magnetic particles for several reasons. For example, the irregular shapes of particles in the aggregated material as seen by TEM are a likely source of uniaxial shape anisotropy. Residual stresses from cation vacancy disorder in maghemite can yield a uniaxial stress anisotropy. Also, surface effects from the reduced size of our particles, the larger fraction of surface atoms, and the

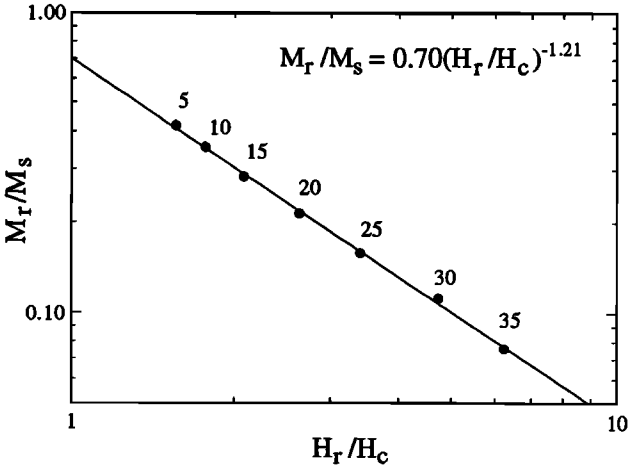

Figure 9. Bilogarithmic Day plot of M_r/M_s versus H_r/H_c. The solid line is the best fit to the equation $M_r/M_s=a(H_r/H_c)^b$ with a=0.70 and b=-1.21. The numbers next to each data point is the measurement temperature (kelvins).

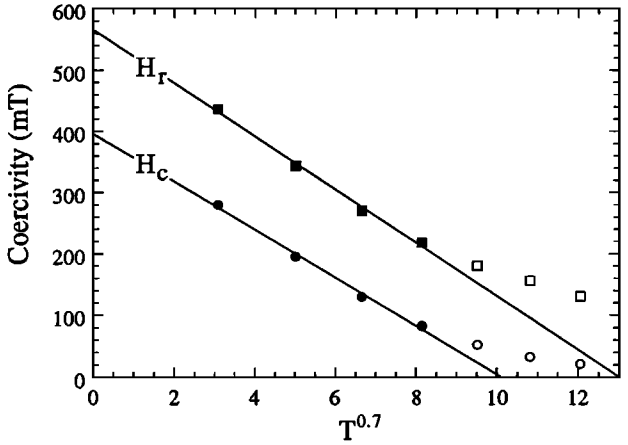

Figure 10. Coercivity (H_c) and coercivity of remanence (H_r) plotted as a function of $T^{0.7}$. Solid lines are the best fit lines to equation (4) in the text for data below 25 K (represented by solid symbols).

heterogeneity of the iron sites at the inorganic-organic interface can give rise to surface anisotropy that can lower the symmetry of the intrinsic, cubic anisotropy. It is likely that a combination of all these factors produces the uniaxial anisotropy in the magnetoferritin particles.

4.8. Thermal Fluctuation Analysis

The temperature dependence of H_c and H_r are plotted in Figure 10 as a function of $T^{0.7}$ following (4) [*Dunlop*, 1976; *Pfeiffer*, 1990]. Both coercivity parameters were used to provide estimates of the anisotropy field. The mean coercivity (H_{c0} or H_{r0}) and <V> were calculated from the intercepts and slopes of the best-fitting lines through the data for temperatures below 25 K ($\approx T_b$), assuming that both the anisotropy field (H_K) and M_s are constant within this temperature range and that M_s=420 kA/m at T=0 K [*Bate*, 1980]. The resulting fit to (4) yields

d=10.3 nm and H_{c0}=39.6 mT
d=10.4 nm and H_{r0}=56.6 mT

The average particle sizes calculated from both coercivity sets are nearly identical and are approximately the same as the estimate obtained from the Langevin fit of the magnetization data at 300 K. Like the room temperature results, hysteresis behavior above 5 K is dominated by the aggregated material. From the mean coercivities calculated from the intercepts in Figure 10, the anisotropy constant can be determined from H_{c0}, $H_{r0} \approx K/M_s$, yielding values of 1.7×10^4 J/m^3 and 2.4×10^4 J/m^3 from the H_c and H_r data, respectively. Although there are no data for the magnetocrystalline anisotropy constant for maghemite at low temperatures, the calculated anisotropy constants are larger than the bulk value of K_1 at 300 K ($K_1=0.45\times10^4$ J/m^3 [*Bate*, 1980]). This, together with the experimental value of $M_r/M_s \approx 0.5$ at 5 K, confirms that a uniaxial-type anisotropy makes the most important contribution to the anisotropy of the magnetoferritin. Finally, the ratio of the two anisotropy fields is 1.43, which is similar to the value obtained from the extrapolated H_r/H_c ratio from the Day plot and higher than the theoretical value of 1.09.

4.9. Calculation of the Frequency Factor

The frequency factor f_0 can be obtained directly from (1) following the procedure given by *Dickson et al.* [1993]. This method uses the observed difference in median blocking temperatures obtained from SIRM (T_{b2}=18 K) and Mössbauer (T_{b1}=300±10 K) data measured on the same sample, which is a consequence of the difference in the characteristic measurement time-scales between the two techniques. We also assume that the effects of interactions on T_b are negligible for both SIRM and Mössbauer measurements, even though both sets of measurements provide median blocking temperatures for the aggregated clusters. From (1), f_0 is given by

$$f_0 = [(t_1)^{\beta}/(t_2)^{\alpha}]^{1/(\alpha-\beta)} \quad (7)$$

where $\beta=T_{b2}/T_{b1}=0.06$, $\alpha=\Delta E_2/\Delta E_1$, and the subscripts 1 and 2 refer to the Mössbauer and magnetization measurements, respectively. By setting $t_1=5\times10^{-9}$ s and t_2=100 s, and assuming that the mean anisotropy barrier is the same for both measurements (α=1), $f_0=9.1\times10^8$ Hz.

The mean energy barriers sampled by the two experimental techniques may not necessarily be the same but could differ slightly as a result of temperature-dependent anisotropy or dipolar interaction effects (α>1). If we decrease or increase α from unity by 10% in order to take into account any differences between the energy barriers sampled by the two techniques, f_0 changes only marginally to 7.9×10^8 Hz (α=1.1) or 10.8×10^8 Hz (α=0.9). A slightly larger variation in f_0 occurs if we change the characteristic Mössbauer time (t_2) used in the calculation. For example, if t_2 equals 10^{-8} s or 10^{-9} s, then f_0 becomes 4.3×10^8 Hz or 50×10^8 Hz, respectively.

The calculated value of $f_0 \approx 10^9$ Hz for the maghemite cores in magnetoferritin agrees well with $f_0=1.1\times10^9$ Hz for magnetite based only on Mössbauer data [*McNab et al.*, 1968]. However, our value for magnetoferritin is a factor of 10^3 lower than f_0 determined for native ferritin using measurement techniques identical to those in the present study [*Dickson et al.*, 1993]. The effects of interparticle interactions in magnetoferritin cannot be the explanation for this difference because interactions will make the calculated f_0 closer in magnitude to the value in native ferritin for the following reason. Interactions tend to increase the blocking temperature and anisotropy energy determined by the magnetization measurements, making both α and β anomalously higher. The combined effect would then make the calculated value of f_0 higher than what would be expected for a noninteracting system. It is unlikely that dipolar interactions are significant in native ferritin because of the much lower particle magnetization of the antiferromagnetic core. A possible explanation for the difference in the values of f_0 may be related to the different types of magnetic spin ordering and anisotropy of the core materials in the two varieties of ferritin: ferrimagnetic in magnetoferritin and antiferromagnetic with uncompensated surface spins in native ferritin.

4.10. Superparamagnetic-Single Domain Transition Size at 5 and 300 K

Using our value for f_0, the mean particle size obtained from the room temperature magnetization data (Figure 4), and T_{b2} from the decay of low temperature remanence

(Figure 5), the anisotropy constant can be determined from (2) to be 1.2×10^4 J/m^3. This value for K is less than that estimated from thermal fluctuation analysis (Figure 10), but this is to be expected. Thermal fluctuation analysis is sensitive to particles with the largest V and H_K whose blocking temperatures have not been exceeded and excludes the finest SPM particles which make up about 16% of the sample at 5 K. By contrast, the thermal decay of SIRM provides averages within the blocking temperature range in which half of the particles have already unblocked. Additionally, some amount of disagreement is expected because the two different measurement techniques provide different measures of the central tendencies of the volume-anisotropy distributions. For instance, the decay of SIRM gives the median value of anisotropy, whereas thermal fluctuation analysis gives the mean value. In an asymmetric distribution skewed towards the right, such as the distribution of observed particle diameters (Figure 1) or the distribution of the intrinsic Stoner-Wohlfarth anisotropy fields for random easy axes, the mean will be less than the median as is experimentally observed. For the purposes of our calculations, the simplest approximation is to assume that $K=1.2\text{-}2.4 \times 10^4$ J/m^3 and that both sets of experiments give a measure of the variation in K.

Once the anisotropy constant is known for our particle size distribution, the SPM transition size can be estimated at any temperature from (2) assuming that K is due to shape anisotropy and varies with temperature as M_s^2. Alternatively, if K is due to stress anisotropy, its temperature dependence would be proportional to the magnetostriction constant and would likely vary less strongly with temperature than shape anisotropy between 5 and 300 K. However, the temperature dependence of magnetostriction in maghemite within the investigated temperature range is unknown; thus it will assumed to be independent of temperature. It is also assumed that K is independent of particle size and would be the same for particles with the same shape but with sizes greater than the largest sized particles in our distribution. This assumption is valid as long as there is no significant surface anisotropy in the magnetoferritin particles.

Regardless of the particular method used to obtain the estimate of K and its temperature dependence, the extrapolated SPM transition size at 300 K using the extreme limits for the anisotropy constant is within a narrow size range of 20-27 nm. This SPM transition size agrees well with room temperature frequency-dependent susceptibility measurements obtained from sized, synthetic maghemite samples between 12 and 50 nm [*Dearing et al.*, 1996], where a pronounced frequency dependence in susceptibility, characteristic of SPM particles, was observed only in particle sizes below 31 nm. In contrast, micromagnetic calculations by *Lyberatos and Chantrell* [1990] predicted the SPM transition size at room temperature for maghemite with cubic magnetocrystalline anisotropy to be 42 nm (for a sphere with the same volume as the cube used in their model), significantly higher than the experimentally determined value for magnetoferritin. The difference is readily explained by the higher uniaxial anisotropy in the magnetoferritin particles compared to the bulk magnetocrystalline anisotropy of maghemite used in the numerical model.

The SPM transition size associated with the lower blocking temperature component (≈60 K) deduced from the Mössbauer measurements in Figure 3 can be estimated using the blocking condition $KV=1.6kT_b$ and the estimated values of K. This gives a blocking diameter of 4.8-6.1 nm, which is indistinguishable from the average size of the discrete particles (6±1 nm) obtained by TEM. Similarly, the blocking temperature for a 4.8 to 6.1 nm-sized particle for a dc measurement is ≈4 K. This is consistent with the SIRM and hysteresis measurements that show that a significant fraction (16%) of the particles are still superparamagnetic at 5 K.

5. Discussion and Conclusions

A magnetic and Mössbauer study of magnetoferritin was carried out over a temperature range from 5 to 350 K. Several different types of magnetization measurements show that the magnetoferritin sample is a weakly interacting suspension of SPM particles of maghemite with a median blocking temperature of 18 K and a magnetic particle size of 10.1 nm. The mean magnetic particle size is larger than the average core size of the discrete ferritin cores (6±1 nm) measured with TEM but consistent with the mean size of the particles within the aggregated clusters of ferritin nanoparticles (10±2.6 nm).

Our main conclusions are the following:

1. The nanoparticles residing within the intact protein cavity of magnetoferritin are superparamagnetic over dc measurement time scales at all temperatures above 5 K. This means that remanence and hysteresis behavior above 5 K must be associated with the larger-sized particles associated with the aggregated material.

2. The preexponential frequency factor f_0 in the Néel relaxation equation was determined from the difference in blocking temperatures measured by dc magnetization and Mössbauer spectroscopy. The value obtained was $f_0=10^9$ Hz, which is in agreement with the order-of-magnitude theoretical estimates of Néel and Brown and is the standard value used in most fine-particle magnetism studies including rock magnetism. This value also justifies the usual SPM blocking condition for dc magnetic measurements obtained from (2) as $KV=25kT$.

3. If the observed experimental difference in f_0 between magnetoferritin and native ferritin is related to the type of magnetic ordering of the core mineral, then the higher value of $f_0=10^{12}$ Hz obtained for the ferrihydrite cores in native ferritin [*Dickson et al.*, 1993] may be more appropriate for antiferromagnetic materials like hematite and goethite. For these minerals, the SPM blocking condition then becomes $KV=32kT$.

4. The superparamagnetic threshold size at room temperature for maghemite for a dc magnetization measurement was estimated to be 20-27 nm. The effects of interactions within the aggregate clusters may make the calculated SPM threshold size somewhat lower than would be expected if the clusters were not interacting because of the increase in blocking temperature produced by particle interactions. Nevertheless, weakly interacting magnetoferritin may be a good analogue for maghemite particles in soils, which do show various degrees of magnetic interactions [e.g., *Maher and Taylor*, 1988].

5. The extrapolated SD value at 0 K for H_r/H_c is 1.32. This value is larger than the theoretical value of 1.09 (also at 0 K) for a Stoner-Wohlfarth particle with uniaxial anisotropy. The experimental value of H_r/H_c may be more appropriate for weakly interacting systems.

Acknowledgments. R.B.F. was supported by NIH grant ROI DK36799-06A4. K.K.W.W. was supported by the BBSRC (U.K.). The Institute for Rock Magnetism (IRM) is supported by grants from the Keck Foundation and the NSF. IRM contribution 9704.

References

Banerjee, S.K., C.P. Hunt, and X.-P. Liu, Separation of local signals from the regional paleomonsoon record of the Chinese Loess Plateau: A rock-magnetism approach, *Geophys. Res. Lett., 20*, 843-846, 1993.

Bate, G., Recording materials, in *Ferromagnetic Materials*, vol. 2, edited by E.P. Wohlfarth, pp. 382-507, North-Holland, New York, 1980.

Bean, C.P., and J.D. Livingston, Superparamagnetism, *J. Appl. Phys., 30, suppl.*, 120S-129S, 1959.

Bell, S.H., M.P. Weir, D.P.E. Dickson, J.F. Gibson, G.A. Sharp, and T.J. Peters, Mössbauer spectroscopic studies of human haemosiderin and ferritin, *Biochim. Biophys. Acta, 787*, 227-236, 1984.

Boas, J.F., and B. Window, Mössbauer effect in ferritin, *Aust. J. Phys., 19*, 573-576, 1966.

Brown, W.F., Jr., Relaxation behavior of fine particles, *J. Appl. Phys., 30*, 1305-1325, 1959.

Bulte, J.W., T. Douglas, S. Mann., R.B. Frankel, B.M. Moskowitz, R.A. Brooks., C.D. Baumgarner, J. Vymazal, M-P. Strub, and J.A. Frank, Magnetoferritin: Characterization of a novel superparamagnetic MR contrast agent, *J. Magn. Reson. Imaging, 4*, 497-505, 1994.

Chantrell, R.W., M. El-Hilo, and K. O'Grady, Spin-glass behavior in a fine particle system, *IEEE Trans. Magn., 27*, 3570-3578, 1991.

Cisowski, S., Interacting vs. non-interacting single domain behavior in natural and synthetic samples, *Phys. Earth Planet. Int., 26*, 56-62, 1981.

Day, R., M.D. Fuller, and V. A. Schmidt, Hysteresis properties of titanomagnetites: Grain size and composition dependence, *Phys. Earth Planet. Inter., 13*, 260-266, 1977.

Dearing, J.A., R.J.L. Dann, K. Hay, J.A. Lees, P.J. Loveland, B.A. Maher, and K. O'Grady, Frequency-dependent susceptibility measurements of environmental materials, *Geophs. J. Int., 124*, 228-240, 1996.

Dickson, D.P.E., N.M.K. Reid, C. Hunt, H.D. Williams, M. El-Hilo and K. O'Grady, Determination of f_0 for fine magnetic particles, *J. Magn. Magn. Mater., 125*, 345-350, 1993.

Dickson, D.P.E, S.A. Walton, S. Mann, and K. Wong, Properties of magnetoferritin: a novel biomagnetic nanoparticle, *Nanostruct. Mater., 9*, 595-599, 1997.

Dunlop, D.J., Theory of the magnetic viscosity of lunar and terrestrial rocks, *Rev. Geophys., 11*, 855-901, 1973.

Dunlop, D.J., Thermal fluctuation analysis: A new technique in rock magnetism, *J. Geophys. Res., 81*, 3511-3717, 1976.

Dunlop, D. J., Magnetism in rocks, *J. Geophys. Res., 100*, 2161-2174, 1995.

El-Hilo, M., K. O'Grady, and R.W. Chantrell, Susceptibility phenomena in a fine particle system, I., Concentration dependence of the peak, *J. Magn. Magn. Mater., 114*, 295-306, 1992.

Gider, S., D.D. Awschalom, T. Douglas, K. Wong, S. Mann, and G. Cain, Classical and quantum magnetism in synthetic ferritin proteins, *J. Appl. Phys., 79*, 5324-5326, 1996.

Gittleman, J.I., B. Abelas, and S. Bozowski, Superparamagnetism and relaxation effects in granular Ni-SiO_2 and Ni-Al_2O_3 films, *Phys. Rev., B, 9*, 3891-3902, 1974.

Henkel, O., Remanenzverhalten und Wechselwirkungen in hartmagnetischen Teilchenkollektiven, *Phys. Status. Solidi., 7*, 919-924, 1964.

Joffe, I., and R. Heuberger, Hysteresis properties of distributions of cubic single-domain ferromagnetic particles, *Philos. Mag., 314*, 1051-1059, 1974.

Kundig, W., and R.S. Hargrove, Electron hopping in magnetite, *Sol. State Commun., 7*, 223-227, 1969.

Lyberatos, A., and R.W. Chantrell, Calculation of the size dependence of the coercive force in fine particles, *IEEE Trans. Magn., 26*, 2119-2121, 1990.

Maher, B.A., and R.M. Taylor, Formation of ultrafine-grained magnetite in soils, *Nature, 336*, 368-370, 1988.

McNab, T.K., R.A. Fox, and A.J.F. Boyle, Some magnetic properties of magnetite (Fe_3O_4) microcrystals, *J. Appl. Phys., 39*, 5703-5711, 1968.

Meldrum, F.C., B.R. Heywood, and S. Mann, Magnetoferritin: In vitro synthesis of a novel magnetic protein, *Science, 257*, 522-523, 1992.

Moon, T., and R.T. Merrill, Single-domain theory of remanent magnetization, *J. Geophys. Res., 93*, 9202-9210, 1988.

Moskowitz, B.M., R.B. Frankel, D.A. Bazylinski, H.J. Jannasch, and D.R. Lovely, A comparison of magnetite particles produced anaerobically by magnetotactic and dissimilatory iron-reducing bacteria, *Geophys. Res. Lett., 16*, 665-668, 1989.

Néel, L., Théorie du trainage magnétique des ferromagnétiques en grains fins avec applications aux terres cuites, *Ann. Geophys, 5*, 99-136, 1949.

Pankhurst, Q.A., S. Betteridge, D.P.E. Dickson, T. Douglas, S. Mann, and R.B. Frankel, Mössbauer spectroscopic and magnetic studies of magnetoferritin, *Hyperfine Inter., 91*, 847-851, 1994.

Pankhurst, Q.A., and R.J. Pollard, Fine-particle magnetic oxides, *J. Phys. Condens. Matter., 5*, 8487-8508, 1993.

Pfeiffer, H., Determination of anisotropy field distribution in particle assemblies taking into account thermal fluctuations, *Phys. Status. Solidi., A, 118*, 295-306, 1990.

Söffge, F., and E. Schmidbauer, Ac susceptibility and static magnetic properties of an Fe_3O_4 ferrofluid, *J. Magn. Magn. Mater., 24*, 54-66, 1981.

Spratt, G.W.D., P.R. Bissell, R.W. Chantrell, and E.P. Wohlfarth, Static and dynamic experimental studies of particulate recording media, *J. Magn. Magn. Mater., 75*, 309-318, 1988.

Stacey, F.D., and S.K. Banerjee, *The Physical Principles of Rock Magnetism*, 195 pp., Elsevier, New York, 1974.

Stoner, E.C., and E.P. Wohlfarth, A mechanism of magnetic hysteresis in heterogeneous alloys, *Philos. Trans. R. Soc. London, Ser. A., 240*, 599-642, 1948.

Tarduno, J.A., Superparamagnetism and reduction diagenesis in pelagic sediments: Enhancement or depletion, *Geophys. Res. Lett., 22*, 1337-1340, 1995.

Tauxe, L., T.A.T. Mullender, and T. Pick, Potbellies, wasp-waists, and superparamagnetism in magnetic hysteresis, *J. Geophys. Res., 101*, 571-583, 1996.

Wohlfarth, E.P., Relations between different modes of acquisition of the remanent magnetization of ferromagnetic particles, *J. Appl. Phys., 29*, 595-596, 1958.

Xiao, G., S.H. Liou, A. Levey, J.N. Taylor, and C.L. Chien, Magnetic relaxation in Fe-(SiO_2) granular films, *Phys. Rev. B, 34*, 7573-7577, 1986.

D. P. E. Dickson and S. A. Walton, Department of Physics, University of Liverpool, Liverpool L69 3BX, England, U.K. (e-mail: Dominic.Dickson@liverpool.ac.uk; S.A.Walton@liverpool.ac.uk)

T. Douglas, S. Mann, and K. K. W. Wong, School of Chemistry, University of Bath, Bath BA2 7AY, England, U.K.

R. B. Frankel, Physics Department, California Polytechnic State University, San Luis Obispo, CA 93407. (e-mail: rfrankel@oboe.aix.calpoly.edu)

B. M. Moskowitz, Department of Geology and Geophysics, Institute for Rock Magnetism, University of Minnesota, 100 Union Street, S.E., Minneapolis, MN 55455. (e-mail: bmosk@maroon.tc.umn.edu)

(Received January 7, 1997; revised May 30, 1997;
accepted June 5, 1997.)